Biochemical Pharmacology 229 (2024) 116469

Contents lists available at ScienceDirect

Biochemical Pharmacology

journal homepage: www.elsevier.com/locate/biochempharm

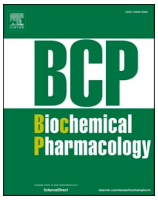

Deregulation of lactate permeability using a small-molecule transporter (Lactrans-1) disturbs intracellular pH and triggers cancer cell death

Alain Arias-Betancur [a,b,c], Pere Fontova [a,d], Daniel Alonso-Carrillo [d], Israel Carreira-Barral [d], Janneke Duis [a,e], María García-Valverde [d], Vanessa Soto-Cerrato [a,b], Roberto Quesada [d,*], Ricardo Pérez-Tomás [a,b,**]

[a] Department of Pathology and Experimental Therapeutics, Faculty of Medicine and Health Sciences, Universitat de Barcelona, 08907, L'Hospitalet de Llobregat, Barcelona, Spain
[b] Molecular Signalling, Oncobell Program, Institut d'Investigació Biomèdica de Bellvitge (IDIBELL), 08908, L'Hospitalet de Llobregat, Barcelona, Spain
[c] Department of Integral Adult Dentistry, Research Centre for Dental Sciences (CICO), Dental School, Universidad de La Frontera, 4811230 Temuco, Chile
[d] Departamento de Química, Facultad de Ciencias, Universidad de Burgos, 09001 Burgos, Spain
[e] Avans University of Applied Science, 4818 AJ Breda, the Netherlands

ARTICLE INFO

Keywords:
Lactate
Anionophores
Click-tambjamines
Cancer metabolism
pH deregulation
Small molecules

ABSTRACT

Due to the relevance of lactic acidosis in cancer, several therapeutic strategies have been developed targeting its production and/or regulation. In this matter, inhibition approaches of key proteins such as lactate dehydrogenase or monocarboxylate transporters have showed promising results, however, metabolic plasticity and tumor heterogeneity limits their efficacy. In this study, we explored the anticancer potential of a new strategy based on disturbing lactate permeability independently of monocarboxylate transporters activity using a small molecule ionophore named Lactrans-1. Derived from click-tambjamines, Lactrans-1 facilitates transmembrane lactate transportation in liposome models and reduces cancer cell viability. The results showed that Lactrans-1 triggered both apoptosis and necrosis depending on the cell line tested, displaying a synergistic effect in combination with first-line standard chemotherapeutic cisplatin. The ability of this compound to transport outward lactate anions was confirmed in A549 and HeLa cells, two cancer cell lines having distinct rates of lactate production. In addition, through cell viability reversion experiments it was possible to establish a correlation between the amount of lactate transported and the cytotoxic effect exhibited. The movement of lactate anions was accompanied with intracellular pH disturbances that included basification of lysosomes and acidification of the cytosol and mitochondria. We also observed mitochondrial swelling, increased ROS production and activation of oxidative stress signaling pathways p38-MAPK and JNK/SAPK. Our findings provide evidence that enhancement of lactate permeability is critical for cellular pH homeostasis and effective to trigger cancer cell death, suggesting that Lactrans-1 may be a promising anticancer therapy.

1. Introduction

The production of lactic acid due to the reprogrammed metabolic activity of cancer cells has major consequences for tumor development [1,2]. As the end-product of the glycolytic pathway in the so-called "Warburg effect", lactic acid, which is rapidly dissociated into lactate anions and protons, is the substrate for the metabolic symbiosis occurring between lactate-producing and lactate-consuming cancer cell populations located within the same tumoral mass [3,4]. Furthermore, it has been reported that lactate and protons play important roles in metabolic rewiring processes [5–7] licensing selective advantages that allow cancer cells to proliferate in adverse tumor microenvironment (TME)

Abbreviations: AO, acridine orange; CI, combination index; IC, inhibitory concentration; JNK/SAPK, c-Jun N-terminal kinase/stress-activated protein kinases; LDH, Lactate dehydrogenase enzyme; MCT, monocarboxylate transporter; MTT, 3-(4,5-dimethylthiazol-2-yl)-2,5-diphenyltetrazolium bromide; p38-MAPK, p38 mitogen-activated protein kinase; PARP, poly (ADP-ribose) polymerases; pH_i, intracellular pH; ROS, reactive oxygen species; TME, tumor microenvironment.

* Corresponding author.
** Corresponding author at: Department of Pathology and Experimental Therapeutics, Faculty of Medicine and Health Sciences, Universitat de Barcelona, 08907, L'Hospitalet de Llobregat, Barcelona, Spain.
E-mail addresses: rquesada@ubu.es (R. Quesada), rperez@ub.edu (R. Pérez-Tomás).

https://doi.org/10.1016/j.bcp.2024.116469
Received 14 February 2024; Received in revised form 5 August 2024; Accepted 5 August 2024
Available online 6 August 2024

conditions [8,9]. These metabolic adaptations driven by lactic acidosis (accumulation of lactate in an acidic TME) may also promote uneven responses to chemotherapy and consequently, favor tumor growth [10,11].

The shuttle of lactate and protons between cancer cells having distinct metabolic phenotypes is mediated by the differential expression of monocarboxylate transporters (MCT) 1 and 4 [3,12]. The symporter activity of MCTs and other proton-extruders located at the plasma membrane is responsible for removing excess of acidity derived from increased metabolic fluxes [13–15]. As part of a more complex regulatory system for intracellular pH (pH_i), these transporters are in charge of maintaining distinct organellar and cytoplasmic pH necessary for the proper function of proteins and enzymes [13,15,16]. Their activity also allows the establishment of an alkaline pH_i that is permissive for malignant processes such as cancer cell proliferation, metabolic adaptation and evasion of apoptosis [17]. In this manner, regulation of lactate and protons homeostasis is crucial to support cellular adaptations necessary for tumor evolution.

Numerous anticancer metabolic strategies have been developed to target lactate and pH homeostasis. For example, pharmacological inhibition of MCT-1 to disturb lactate transport has shown promising results by increasing intracellular lactate levels, inhibiting glycolysis and inducing a cytostatic response, with AZD3965 inhibitor being tested in clinical trials [18,19]. On the other hand, ion-homeostasis disturbing agents, such as small molecules with ionophoric activity have shown to effectively induce intracellular acidification and trigger cancer cell death [20]. The effect of these compounds relies mostly on the facilitated transport of chloride, calcium and potassium, and their disturbance usually promotes oxidative environments that trigger the activation of cellular stress signaling pathways and programmed or unprogrammed forms of cell death [21–24]. Thereby, it is feasible to propose that other relevant anions in the specific context of cancer, such as lactate, could be interesting and more specific targets.

We have previously reported a new class of small-molecules (click-tambjamines) that are able to facilitate lactate anion transport in liposome models and living cells [25]. Thus, in this work we explore the molecular mechanisms of action and the anticancer effects of the most potent and selective small-molecule discovered, capable of facilitating lactate transport. We tested this compound against various cell lines covering a wide range of genomic and metabolic backgrounds. We focused on studying expected ionic pH_i disturbances caused by lactate movement and how these events are linked to observed cancer cell death.

2. Material and methods

2.1. Synthesis of compounds

Click-tambjamine derivatives Lactrans-1, −4 and −5 (previously named as compounds 1, 4 and 5, respectively) were synthesized as previously reported (patent application P202330370) [25]. Briefly, synthesis was made by acid-catalyzed condensation of the appropriate amine (1-adamantylamine for Lactrans-1 and −5, and ethanolamine for Lactrans-4) with the corresponding aldehyde (5-(1-(4-(*tert*-butyl) phenyl)-1*H*-1,2,3-triazol-4-yl)-3-methoxy-1*H*-pyrrole-2-carbaldehyde for Lactrans-1, or 5-(1-(2-hydroxyethyl)-1*H*-1,2,3-triazol-4-yl)-3-methoxy-1*H*-pyrrole-2-carbaldehyde, for Lactrans-4 and −5) in boiling chloroform. After treatment with a hydrochloric acid aqueous solution, click-tambjamines were obtained as their hydrochloric salts. Compounds were dissolved at 10 mmol/L in dimethyl sulfoxide (DMSO) and stored at −20 °C until their utilization.

2.2. Cell lines and culture conditions

Human cell lines A549 (lung adenocarcinoma), HeLa (cervix adenocarcinoma), SW620 (colorectal adenocarcinoma), SW900 (lung squamous carcinoma) and MCF10A (non-cancer epithelial breast cells) were obtained from the American Type Culture Collection (ATCC, Manassas, VA, USA). A549, HeLa and SW620 cells were cultured in Dulbecco's Modified Eagle's Medium (DMEM; Biological Industries, Beit Haemek, Israel), while SW900 cells were cultured in Roswell Park Memorial Institute medium (RPMI, Biological Industries). All of them were supplemented with 10 % heat-inactivated fetal bovine serum (FBS; Gibco, Paisley, UK), 100 U/mL penicillin, 100 μg/mL streptomycin, and 2 mM glutamine (all from Biological Industries). In the case of MCF10A, cells were cultured in DMEM/F12 medium supplemented with 5 % horse serum (HS; Gibco), 100 U/mL penicillin, 100 μg/mL streptomycin, 2 mM glutamine (Biological Industries), 0.5 μg/ml hydrocortisone, 20 ng/ml EGF, 100 ng/ml choleric toxin, and 10 μg/ml insulin (Sigma Aldrich, St. Louis, MO, USA). In all the experiments where lactate concentrations were determined, normal FBS or HS was replaced by dialyzed FBS (lactate free). All cell lines were grown at 37 °C in an incubator with 5 % CO_2 atmosphere.

2.3. Cell viability assays

The cytotoxic potential of the synthetized compounds was assessed using the 3-(4,5-dimethylthiazol-2-yl)-2,5-diphenyltetrazolium bromide (MTT, Sigma-Aldrich, Merck KGaA, St Louis, MO, USA) colorimetric assay. Cells were seeded at 10^4 cell/well (90 μl) in 96-well microtiter plates and incubated overnight. The next day, they were treated with Lactrans-1, −4 and −5 at different ranging concentrations (from 0.8 to 23 μmol/L or from 0.8 to 100 μmol/L) or with DMSO as control. Cells were incubated for 24 h and after the treatment period, 10 μL of MTT solution were added (5 mg/mL) and incubated for 2 h at 37 °C. Then, the medium was removed and formazan crystals were dissolved in 100 μL DMSO. Absorbance was read in a spectrophotometer at 570 nm using a multiwell plate reader (Multiskan FC, ThermoFisher Scientific Inc, Whaltman, MA, USA). Cell viability, dose–response curves and inhibitory concentration (IC) values of 25 %, 50 % and 75 % of the cell population were calculated using GraphPad Prism 8.0.1 for Windows (Graph-Pad for Science Inc., San Diego, CA, USA). For combination therapy assays, after seeding as previously described, cells were treated with IC_{50} value of Lactrans-1 for 4 h before adding escalating doses of chemotherapeutic agent cisplatin (50, 100, 150, 200 and 250 μM) for additional 24 h. Thus, the percentages of cell population affected by the single or combination therapy were analyzed with CompuSyn software (version 1.0; ComboSyn, Paramus, NJ, USA) to determine the Combination Index (CI) at different concentrations of chemotherapeutics. CI is used to describe the type of interaction between therapeutic compounds that can be synergistic ($0.30 < CI < 0.70$), moderately synergistic ($0.70 < CI < 0.85$), slightly synergistic ($0.85 < CI < 0.90$), additive ($0.90 < CI < 1.10$) or antagonistic ($CI > 1.10$). For cell viability reversion experiments, A549 and HeLa cells were seeded and cultured for 24 h in DMEM base (powder reconstituted in water; Sigma Aldrich) supplemented with 1 mM of glucose (Sigma-Aldrich) and other nutrients as described above. Next day, cells were treated with Lactrans-1 after an adaptation time (2 h) in fresh media supplemented with 1- or 5-mM glucose, respectively (deprivation condition), before continuing with MTT assay protocol. All data are presented as the mean ± standard deviation (SD).

2.4. Live-Cell imaging

Cytoplasmic morphology of cells was monitored through phase contrast microscopy. Cells were seeded at 1 x 10^5 cells/well (1 mL) in 12-well plates and allowed to grow overnight. The next day, Lactrans-1 treatment was added, and microscopic images were taken at 0, 1, and 4 h using a Leica inverted phase contrast microscope DMIRBE equipped with digital capture software (Leica Microsystems, Wetzlar, Germany). To study the subcellular localization of Lactrans-1, first, a lambda scan analysis was performed using confocal microscopy in A549 cells (seeded at 2 x 10^4 cells/well in an 8-well sterile μ-Slide) treated with 4.9 μM for

1 h. Emission fluorescent intensity was captured every λ = 10 nm between 405 and 720 nm after excitation with 405, 488, 561 and 633 nm lasers. Then, to localize the compound inside the cell, organelle-specific trackers for lysosome (LysoTracker™ Red, Invitrogen, ThermoFisher Scientific, CA, USA) and for mitochondria (MitoTracker™ Deep Red, Invitrogen, ThermoFisher Scientific) were used. Images were taken using a Carl Zeiss LSM 880 spectral confocal laser-scanning microscope (Carl Zeiss Microscopy GmbH, Jena, Germany) and processed with ZEN 2 blue edition software (Zeiss). Finally, alive and dead cells morphology was assessed through a combination of propidium iodide (0.3 μg/mL, incubated 1 h) and Hoechst 33,342 (0.3 μg/mL, incubated 30 min) vital staining. A549 and HeLa cells were seeded at 2 x 10^4 cells/well (200 μL) in an 8-well sterile μ-Slide (Ibidi, Gräfelfing, Germany) and after overnight incubation they were treated with 4.9 and 3.9 μM of Lactrans-1 for 1, 4, 8 and 24 h, respectively.

2.5. Cell death analysis

Cell death was evaluated through flow cytometry using the APC Annexin V/Dead Cell Apoptosis Kit with APC annexin V and Sytox® Green (Molecular Probes, Invitrogen, OR, USA). Briefly, cells were seeded at 2.7 x 10^5 cell/well (2.7 mL) in 6-well plates and incubated overnight. The next day, different cell lines were treated with Lactrans-1 with appropriate doses (dose–response) and times (single point at 24 h and time-course). To inhibit the activation of apoptosis, cells were pre-treated for 4 h with a pan-caspase inhibitor Q-VD-OPh at 20 μM (QVD, Selleckchem, Cologne, Germany). After treatment, non-adherent cells were collected along with attached cells, after their trypsinization. Then, cells were washed, counted and resuspended with binding buffer 1X (50 mM HEPES, 700 mM NaCl, 12.5 mM $CaCl_2$, pH = 7.4) at 10^6 cell/mL. Finally, 100 μL of the cell suspension were mixed with 5 μL of APC Annexin V reagent and 1 μL of 1 μM SYTOX® Green and incubated for 15 min at 37 °C before cell cytometry acquisition using FACS Canto II™ cytometer (Beckton Dickinson, Franklin Lanes, NJ, USA). At least 10,000 events were recorded from each condition to determine the percentages of early apoptotic (Annexin V +/Sytox -) and late apoptotic/dead cells (Annexin V +/Sytox +) populations.

2.6. Extra- and intracellular lactate determination

Extra- and intracellular lactate levels were measured using a luminescent-based method that couples lactate oxidation and NAD^+ reduction with a bioluminescent NADH detection system (Lactate-Glo™ Assay Kit, Promega, Madison, WI, USA). In brief, cells were seeded at 1 x 10^5 cells/well (1 mL) in 12-well plates and incubated overnight. The next day, after treatment incubation with Lactrans-1, −4 and −5, extracellular medium was collected, cells were washed with PBS and then permeabilized with 150 μL HCl diluted in PBS 1X (0.2 M) for 5 min. Intracellular extracts in HCl were neutralized with 50 μL Tris-base (1 M) before incubation with lactate detection reagent (ratio 1:1). Extracellular lactate levels were measured in the medium previously collected. Luminescence was recorded after 1 h of reaction using a FLUORstar OPTIMA plate reader (BMG LabTech, Ortenberg, Germany) and both extra- and intracellular lactate concentrations were determined from a proper standard curve. Lactate levels were normalized to protein content (BCA protein assay kit, Pierce™, Thermo Fisher Scientific Inc.) by lysing cells using SDS (2 % v/v) after collecting intracellular extracts. In some conditions, MCTs were pharmacologically inhibited using Syrosingopine (Syro; 10 μM, pre-treatment for 1 h) to prevent basal lactate shuttle of glycolytic cancer cells.

2.7. Acridine orange staining

Lysosomal pH was assessed using acridine orange (AO) staining, which emission changes from orange, when is protonated in acidic compartments (like lysosomes or late endosomes), to green in other less acidic parts of the cell. First, A549 and HeLa cells were seeded at 1 x 10^5 cell/well (1 mL) in a 12-well plate on glass coverslips and incubated overnight. Afterwards, cells were treated with different doses of Lactrans-1 for 1 h (or with DMSO for control cells). Then, cells were washed twice with PBS 1X, stained with AO solution at 5 μg/mL and incubated for 30 min at room temperature protected from light. After three washes with PBS 1X containing 10 % FBS, the coverslips with stained cells were observed using NIKON eclipse E800 microscope with a 330/380 nm filter (Nikon Europe BV, Badhoevedorp, The Netherlands).

2.8. pH_i determination

pH_i measurement was performed using the pHrodo™ Red AM staining kit (Molecular Probes). A549 and HeLa cells were seeded at 1 x 10^4 cells/well (100 μL) in a 96-well clear bottom black microplate and incubated overnight. The next day, after 1 h of treatment with different doses of Lactrans-1 (or DMSO for controls), cells were washed with an HEPES-based buffer (pH = 7.4) and labelled with pHrodo™ staining solution for 30 min at 37 °C. Finally, staining solution was removed and cells were washed twice with the same buffer before acquiring fluorescent emission (550/590 nm Ex/Em) using a FLUORstar OPTIMA plate reader (BMG LabTech). Quantitative analysis of pH was made using the Intracellular pH Calibration Curve Kit (Molecular Probes). For qualitative assessment of pH_i, fluorescent emission of treated cells was acquired using a Carl Zeiss LSM 880 spectral confocal laser-scanning microscope (Carl Zeiss Microscopy GmbH). In addition, pH assessment of subcellular compartments or organelles was made by dual-staining discrimination using pHrodo™ Red AM and LysoTracker™ Green or MitoTracker™ Deep Red through confocal microscopy. For these experiments, cells were seeded at 2 x 10^4 cells/well (200 μL) in an 8-well sterile μ-Slide (Ibidi).

2.9. Mitochondrial membrane potential

MitoTracker™ Red CMXRos (Molecular Probes) was used to monitor mitochondrial membrane potential in cells through confocal microscopy. A549 cells were seeded at 2 x 10^4 cells/well (200 μL) in an 8-well sterile μ-Slide (Ibidi). After overnight incubation, cells were treated with 4.9 μM of Lactrans-1 for 2, 3 and 4 h and incubated with MitoTracker™ Red CMXRos. Images were captured using a Carl Zeiss LSM 880 spectral confocal laser-scanning microscope (Carl Zeiss Microscopy GmbH).

2.10. Reactive oxygen species quantification

Reactive oxygen species (ROS) formation was assessed using the CellROX® Deep Red Reagent compatible for flow cytometry (Molecular Probes). Briefly, A549 and HeLa cells were seeded at 2.7 x 10^5 cell/well (2.7 mL) in 6-well plates and incubated for 24 h. Next day, cells were treated with the appropriate dose of Lactrans-1 in a time-course experiment (at 30, 60, 120, 180 and 240 min). A positive control for ROS formation named *tert*-butyl hydroperoxide (TBHP; Sigma Aldrich) was used at 2 mM for 1 h. Afterwards, cells were washed with PBS 1X and harvested for staining with CellROX® Deep Red Reagent (final concentration at 750 nM, incubated for 45 min at 37 °C). Additionally, Sytox® Green staining (Molecular Probes) was used to discriminate dead cell populations (final concentration 10 nM, incubated for 15 min at 37 °C before cell cytometry acquisition). Cell cytometry acquisition was performed in a FACS Canto II™ cytometer (Beckton Dickinson) and at least 10,000 events were recorded for each condition.

2.11. Immunoblot analysis

Different cell lines were seeded at 2.7 x 10^5 cell/well (2.7 mL) in 6-well plates and incubated overnight. Next day, cells were treated with appropriate doses of Lactrans-1 in dose–response or time-course

experiments. After treatment, protein extracts were prepared using RIPA lysis buffer (0.1 % SDS, 1 % NP-40 and 0.5 % sodium deoxycholate in PBS) with 40 mM β-glycerophosphate, 50 mM sodium fluoride, 1 mM sodium orthovanadate, 1 mM phenylmethylsulfonyl fluoride and a serine and cysteine protease inhibitor cocktail (Roche, Manheim, Germany). In addition, protein extract of cells cultured in basal conditions (no treatment) were prepared. After protein quantification using BCA protein assay kit (Pierce™, ThermoFisher Scientific Inc), total proteins (25 to 30 μg) were first resolved on SDS-PAGE and then transferred to PVDF membranes (Bio-Rad, Hercules, CA, USA). Then, membranes were blocked for 1 h in 5 % milk diluted in TBS-Tween (50 mM Tris–HCl pH 7.5, 150 mM NaCl, 0.1 % Tween-20) and incubated overnight at 4 °C with the following primary antibodies: anti-PARP (#9542), anti-procaspase 3 (#9662), anti-cleaved caspase 3 (#9664), anti-procaspase 8 (#9746), anti-procaspase 9 (#9502), anti-cleaved caspase 9 (#7237), anti-p38 MAPK (#8690), anti-phospho-p38 MAPK (#4511) (Thr180/Tyr182), anti-JNK/SAPK (#9258), anti-phospho-JNK/SAPK (#4668) (Thr183/Tyr185), anti-mTOR (#2972), and anti-GAPDH (#2118), all from Cell Signaling Technology (Danvers, MA, USA); anti-MCT4 (sc-376140), and anti-actin (sc-1616/sc1615), from Santa Cruz Biotechnology (Dallas, TX, USA); and anti-MCT1 (20139-1-AP) from ProteinTech (Rosemont, IL, USA); anti-RIP1 (610549) from BD Biosciences (Franklin Lakes, NJ, USA); anti-phospho-MLKL (ab187091) (Ser358) from Abcam (Cambridge, UK). Antibody binding was detected using goat anti-mouse IgG-HRP (sc-2005), goat anti-rabbit IgG-HRP (sc-2004) and donkey anti-goat IgG-HRP (A15999) secondary antibodies with ECL detection kit (GE Healthcare, Chicago, IL, USA). GAPDH, Actin and mTOR were used as gel loading controls. Images were captured on an Image Quant™ LAS 500 (GE Healthcare) and band densitometries were retrieved using the software ImageJ v1.52 (National Institutes of Health, Bethesda, MD, USA).

2.12. Statistical analysis

Images and quantitative data were collected from at least three independent experiments. Statistical analysis was performed using GraphPad Prism 8.0.1 software (Graph-Pad for Science Inc.). One-way or Two-way ANOVA with post hoc Tukey's or Sidak's tests for multiple comparison were carried out to compare different groups, respectively, and *t*-student when only two groups were compared. Statistical differences were considered when $p < 0.05$.

3. Results

3.1. Lactrans-1 reduces cancer cell viability through the induction of apoptosis and necrosis

Previously, we were able to demonstrate that the activity of several novel click-tambjamines as transmembrane lactate anion carriers was related to a reduction on cell viability [25]. To further investigate this association, the cytotoxicity of the most promising compound reported, named Lactrans-1 (previously designated as compound 1; Fig. 1), was systematically assessed. For the purpose of mechanistic studies, two other click-tambjamine derivatives named Lactrans-4 and −5 (previously designated as compound 4 and 5, respectively; Fig. 1) were also included in this study as negative controls. Both compounds are structurally very similar to Lactrans-1 yet they display minimal anionophoric and cytotoxic activities.

First, the potential in reducing cancer cell viability of these compounds was extended to a new panel of cell lines that included colon (SW620) and lung (A549 and SW900) cancer cells. In accordance with our previous report, Lactrans-1 displayed cytotoxic activity after 24 h with IC_{50} values ranging from 2.1 to 4.4 μM, while Lactrans-4 and −5 were less harmful and essentially ineffective at the dose range tested (Table 1). These results support a strong correlation between the efficacy of lactate transport and the cytotoxicity of these compounds [25].

To identify which cell death mechanism is activated upon Lactrans-1, a cell death analysis was performed. SW620, HeLa, A549, SW900 and MCF10A cells were treated for 24 h with their corresponding IC_{75} value of Lactrans-1 and analyzed by flow cytometry (Fig. 2A). The results showed a significant increase in both early and late apoptotic/dead cell populations after treatment compared to controls in all cell lines (Fig. 2B). Western blot analysis revealed different ways of apoptosis activation between these cell lines (Fig. 2C): while levels of cleaved PARP increased notoriously right after 8 h of treatment in HeLa and MCF10A cells, it only did after 24 h in SW620, A549 and SW900 cells (Fig. 2D). Additionally, a significant increase of cleaved caspase 3 was found only in SW620, HeLa and SW900 cells after 24 h of treatment. Enhanced expression of cleaved caspase 3 was also observed in MCF10A after 8 h of treatment although it did not reach significance. Flow cytometry and western blot analysis could indicate a strong apoptotic response in cells such as SW620, HeLa, SW900 and MCF10A which is different to the response observed in A549 cells. Based on these differences, A549 and HeLa cells were selected for further analysis of cell death mechanisms.

Next, A549 and HeLa cell lines were treated with 4.9 and 3.9 μM of Lactrans-1, respectively, and the cell population was assessed by flow cytometry in a time-course manner. The results in A549 cells showed a significant amount of cell death as soon as 1 h of treatment, with a predominant late apoptotic/dead cell population (Fig. 3A). Here, an

Table 1
Inhibitory concentrations (ICs) values (in μM) of click-tambjamine Lactrans-1, −4 and −5 in SW620, A549, SW900, HeLa and MCF10A cell lines. ▽ Data extracted from our previous work [25]. All data represent mean ± SD of at least three independent experiments.

Code		SW620	A549	SW900	HeLa▽	MCF10A▽
1	IC_{75}	3.70 ± 0.39	4.92 ± 1.09	5.57 ± 0.59	3.95 ± 0.26	11.22 ± 3.94
	IC_{50}	2.14 ± 0.32	3.35 ± 0.87	4.36 ± 0.27	3.36 ± 0.19	7.66 ± 1.86
	IC_{25}	1.26 ± 0.35	2.30 ± 0.71	3.43 ± 0.06	2.85 ± 0.16	5.36 ± 1.09
4	IC_{75}	>100	>100	>100	>100	>100
	IC_{50}	75.58 ± 6.20	>100	>100	>100	>100
	IC_{25}	37.92 ± 2.36	>100	>100	>100	98.64 ± 0.94
5	IC_{75}	89.87 ± 2.04	>100	>100	93.73 ± 3.71	>100
	IC_{50}	80.83 ± 1.86	>100	>100	85.57 ± 2.94	>100
	IC_{25}	72.72 ± 2.51	>100	>100	78.14 ± 3.00	94.92 ± 5.23

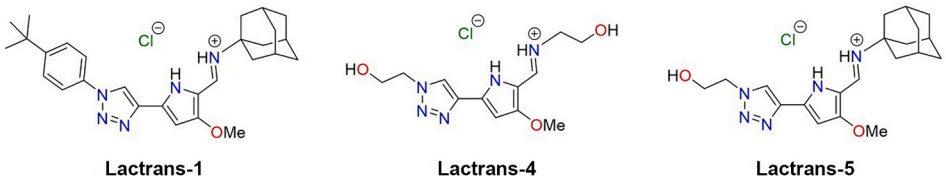

Fig. 1. Click-tambjamine derivatives named Lactrans-1, −4 and −5.

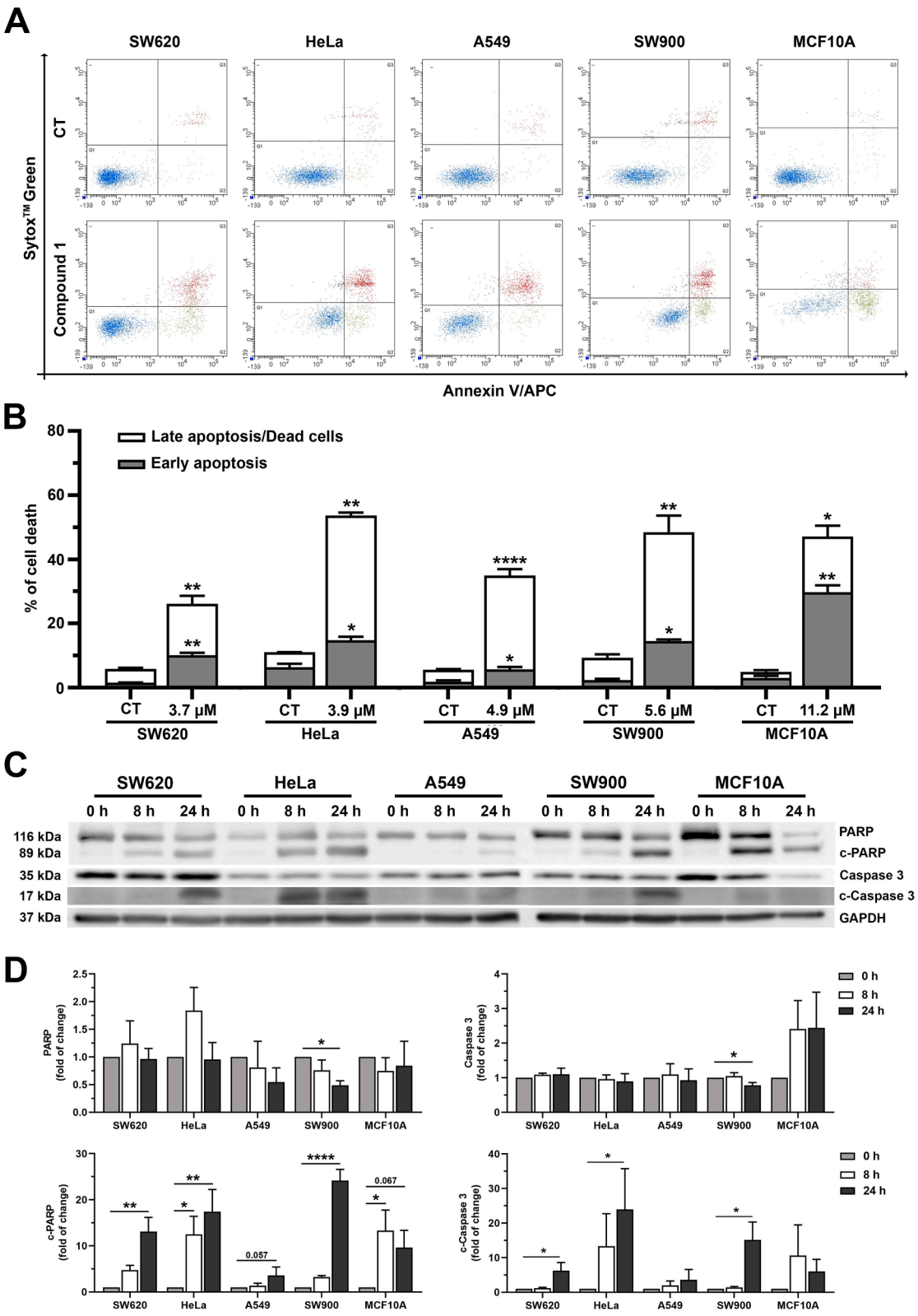

Fig. 2. Cell death characterization in different cell lines (SW620, HeLa, A549, SW900 and MCF10A) treated with Lactrans-1. **A)** Representative plots of flow cytometry analysis of cells treated with their corresponding IC_{75} value for 24 h. Cells were stained with APC annexin V and Sytox™ Green. **B)** Quantification of cell percentages of early (Annexin+/Sytox−) and late apoptotic/dead cells (Annexin+/Sytox+) populations. **C)** Western blot showing apoptotic related proteins in cells treated for 8 and 24 h with same doses of Lactrans-1 as in A). GAPDH expression was used as loading control. **D)** The bar graphs represent expression levels (mean ± SEM) of apoptotic-related proteins (showed in C) expressed as a fold of change against time 0 h. At least three independent experiments were performed. * $p < 0.05$, **$p < 0.01$, and **** $p < 0.0001$ indicate significant differences compared to time 0 h.

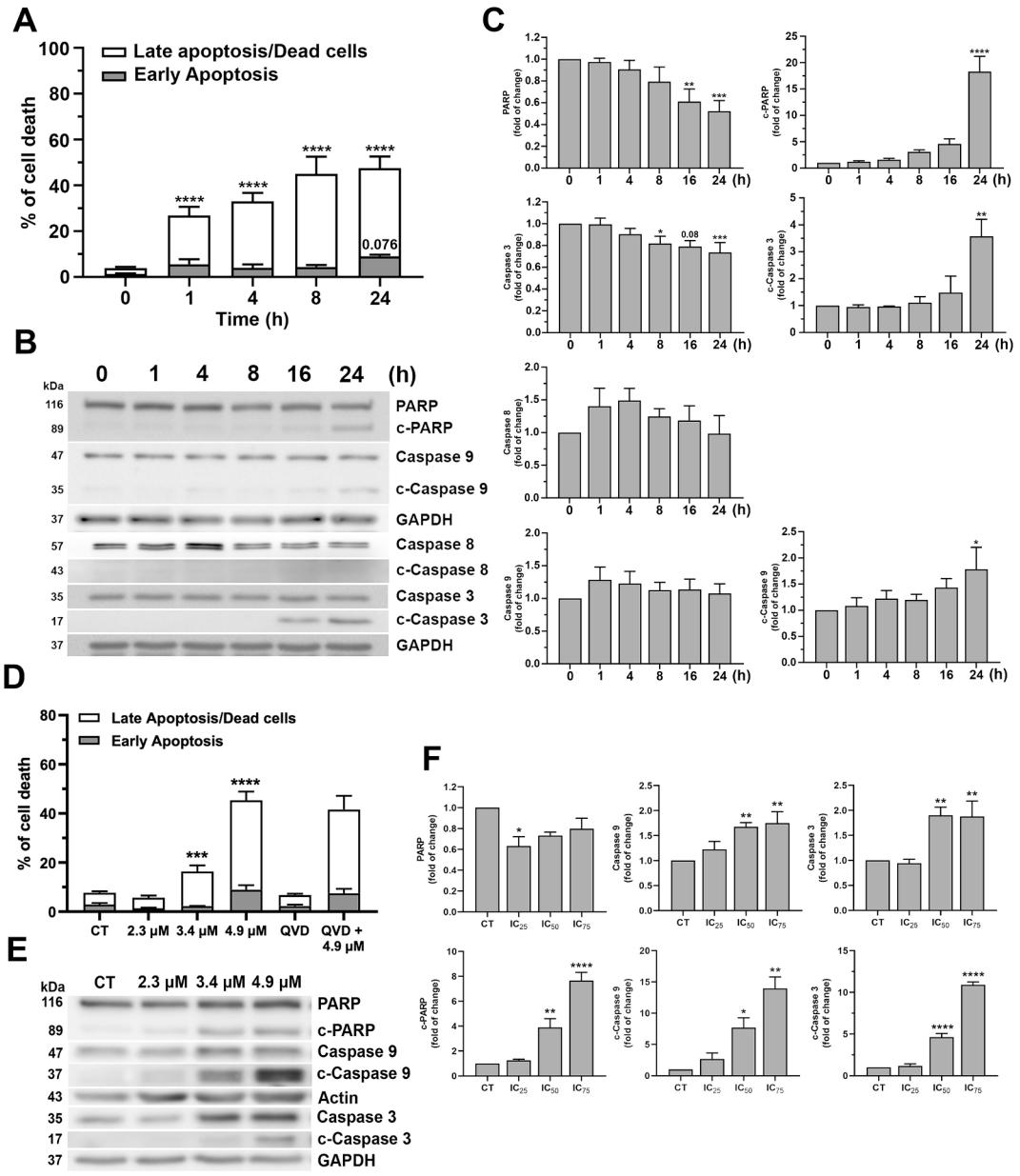

Fig. 3. Cell death analysis in A549 cells. **A)** and **D)** Flow cytometry analysis of cells treated in a time-course (using 4.9 µM of Lactrans-1) and dose–response (at 24 h of treatment) manner, respectively. Q-VD-Oph (QVD) pre-treatment (20 µM during 4 h) was used in order to inhibit caspases activation. After treatment, cells were stained with APC annexin V and Sytox® Green and the percentages of early (Annexin+/Sytox−) and late apoptotic/dead cells (Annexin+/Sytox+) were quantified. **B)** and **E)** Western blot showing apoptotic-related proteins of cells treated in A) and D). GAPDH or Actin expression were used as loading controls, respectively. **C)** and F) The bar graphs represent expression levels (mean ± SEM) of apoptotic-related proteins (showed in B and E) expressed as a fold of change against time 0 h or control (CT), respectively. At least three independent experiments were performed * $p < 0.05$, ** $p < 0.01$, *** $p < 0.001$ and **** $p < 0.0001$ indicate significant differences compared to time 0 h or control (CT), respectively.

almost significantly higher percentage of early apoptotic cells was observed only after 24 h of treatment ($p = 0.076$). This was confirmed by western blot showing a slight but significant increase in protein expression of cleaved PARP, cleaved caspase 3 and cleaved caspase 9 at 24 h (Fig. 3B and C). In these cells, the expression of procaspase 8 was not diminished, and its cleaved form was not detected. In addition, a dose-dependent activation of apoptosis was observed at 24 h since the expression of cleaved PARP, and cleaved caspases 3 and 9 were only increased at higher doses (Fig. 3D, E and F). Furthermore, the dead cell population after pre-treatment with the pan-caspase inhibitor (QVD) did not decrease. This result confirmed that the cell death observed in A549 cells by Lactrans-1 was not mainly caused by caspases activation related with the apoptotic pathway (Fig. 3D).

Meanwhile, in HeLa cells flow cytometry analysis revealed an increase of total cell death along time with significantly higher percentages starting 4 h after treatment (Fig. 4A). These findings were confirmed by western blot, in which protein expression of PARP and procaspase 3 slightly decreased over time, while their cleaved forms significantly increased after 16 h (Fig. 4B and C). Moreover, expression of cleaved caspases 9 and 8 was significantly higher compared to control after 8 and 16 h, respectively (Fig. 4B and C). A dose-dependent effect was observed after treatment with different doses of Lactrans-1 for 24 h, since the expression of cleaved PARP, and cleaved caspases 3 and 9 were significantly higher at the highest dose (Fig. 4D, E and F). Moreover, a significant decrease in the late apoptotic cell population after QVD pre-treatment (Fig. 4D) was observed, corroborating the implication of the

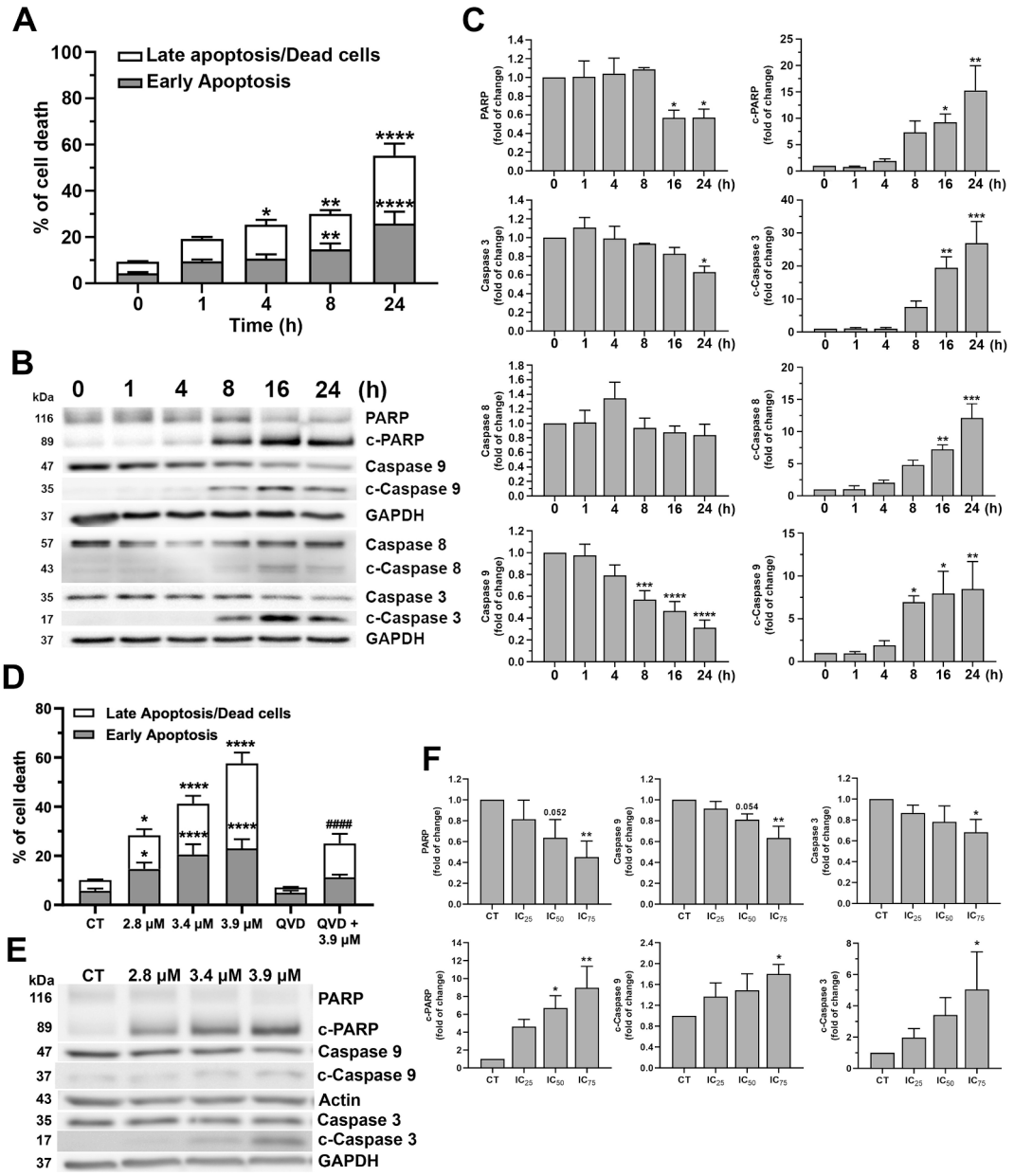

Fig. 4. Cell death analysis in HeLa cells. **A) and D)** Flow cytometry analysis of cells treated in a time-course (using 3.9 µM of Lactrans-1) and dose–response (at 24 h of treatment) manner, respectively. Q-VD-Oph (QVD) pre-treatment (20 µM during 4 h) was used in order to inhibit caspases activation. After treatment, cells were stained with APC annexin V and Sytox® Green and the percentages of early (Annexin+/Sytox−) and late apoptotic/dead cells (Annexin+/Sytox+) were quantified. **B) and E)** Western blot showing apoptotic-related proteins of cells treated in A) and D). GAPDH or Actin expression were used as loading controls, respectively. **C) and F)** The bar graphs represent expression levels (mean ± SEM) of apoptotic-related proteins (showed in B and E) expressed as a fold of change against time 0 h or control (CT), respectively. At least three independent experiments were performed * $p < 0.05$, ** $p < 0.01$, *** $p < 0.001$ and **** $p < 0.0001$ indicate significant differences compared to time 0 h or control (CT), respectively.

apoptotic pathway in the cell death induced by Lactrans-1.

To investigate the differences observed between these two cell lines, morphological features of cell death were analyzed through confocal microscopy. Images revealed that upon Lactrans-1 treatment, HeLa cells showed typical apoptotic features such as nuclear condensation/fragmentation, blebbing and appearance of apoptotic bodies (Fig. 5A). This and our previous results confirmed that apoptosis is the main cell death mechanism triggered by Lactrans-1 in these cells. On the other hand, images of A549 cells showed mainly membrane swelling and intracellular leakage, which is indicative of necrosis or necroptosis (Fig. 5A). To support these observations, western blot analysis targeting two key proteins of the necroptosis mechanism, RIPK1 and phospho-MLKL were performed (Fig. 5B) in these cells. Our results showed a lack of increase in both proteins, thus, discarding necroptosis as the cell death mechanism induced by Lactrans-1.

3.2. *Lactate anion exportation by Lactrans-1 in cancer cells promotes cell death*

In order to select an appropriate *in vitro* model to study lactate permeability, we assessed basal lactate production rate and expression of lactate-proton symporter MCT in all previously tested cell lines. The results showed that HeLa and the non-cancerous cells MCF10A produced higher amounts of lactate with also higher expression of both MCT-1 and −4 isoforms compared to the rest of cells (Fig. 6A, B and C). Considering these results, once more A549 and HeLa cells were selected for the

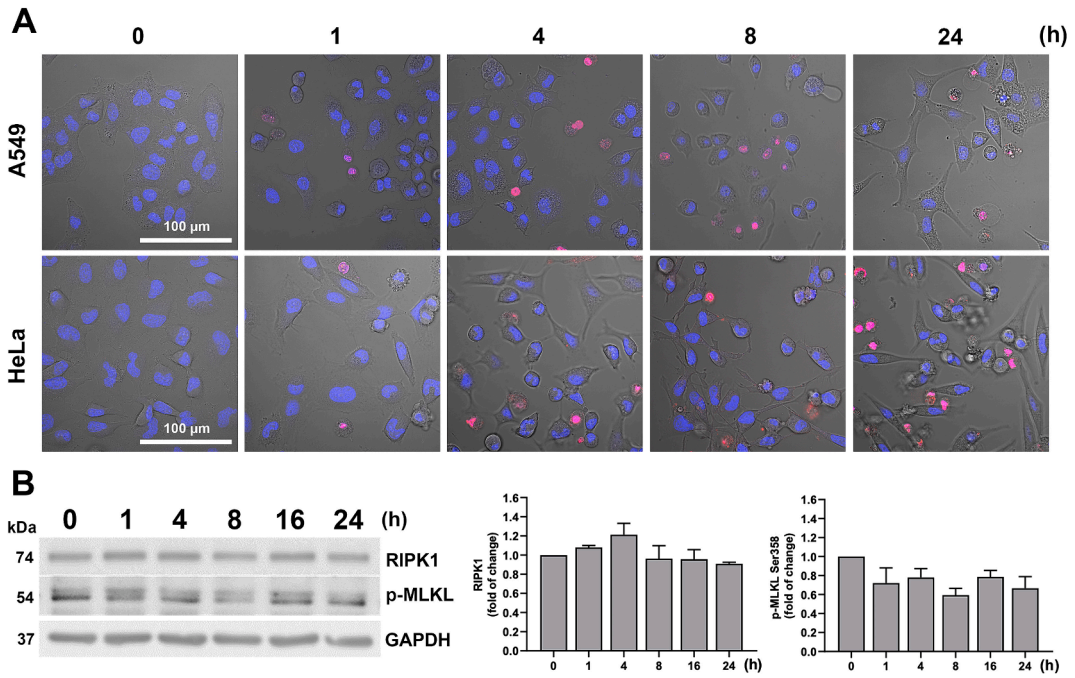

Fig. 5. Cell death analysis in cells treated with Lactrans-1. A) HeLa and A549 cells were treated for 1, 4, 8 and 24 h with 3.9 and 4.9 µM, respectively. After treatment, cells were stained with vital dyes Hoechst and Propidium Iodide. Images were taken using confocal microscopy. B) Western blot showing necroptosis-related proteins in A549 cells treated in a time-course manner using 4.9 µM of Lactrans-1. GAPDH expression was used as loading control. The bar graphs represent expression levels (mean ± SEM) of necroptosis-related proteins expressed as a fold of change against time 0 h. Three independent experiments were performed.

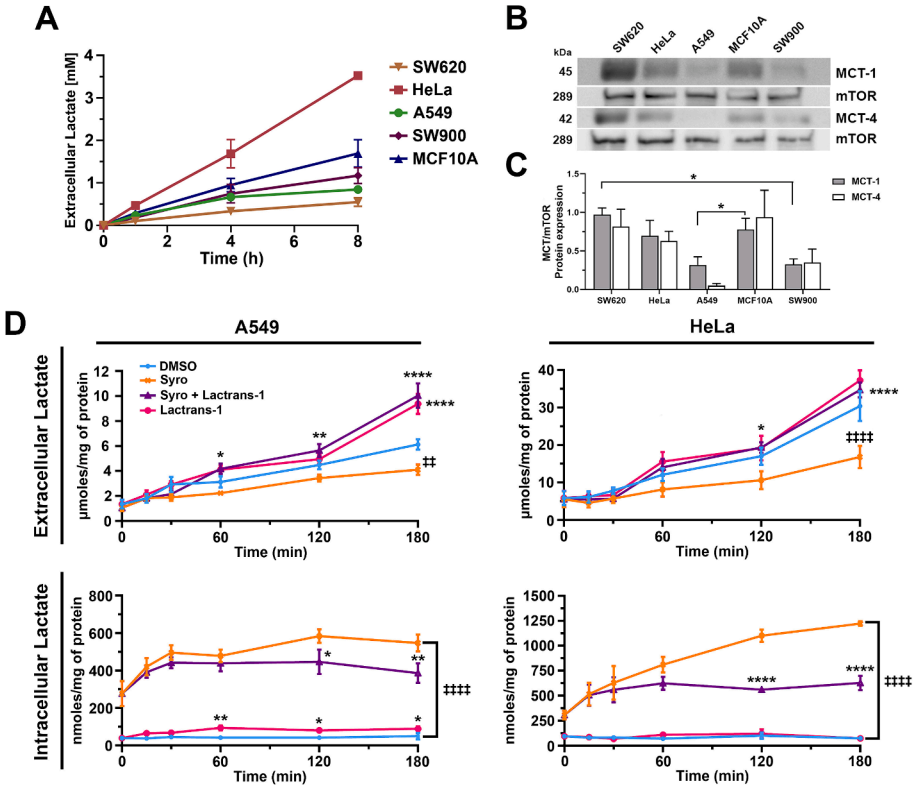

Fig. 6. Lactate determination in A549 and HeLa cells treated with Lactrans-1. **A)** Lactate production curves (up to 8 h) of SW620, HeLa, A549, SW900 and MCF10A cell lines cultured in corresponding media supplemented with 10 mM glucose. **B)** Western blot showing protein expression of MCT-1 and MCT-4 in SW620, HeLa, A549, SW900 and MCF10A cell lines. mTOR was used as loading control. **C)** The bar graphs represent expression levels (mean ± SEM) of MCT-1 and −4 normalized by the relative expression of mTOR. At least three independent experiments were performed. **D)** Extra- and intracellular lactate levels were determined in A549 and HeLa cells treated with Lactrans-1 in a time-course experiment using 2.3 and 2.8 µM, respectively. Here, normal lactate shuttle by MCTs was inhibited using Syro (10 µM, pre-treated for 1 h). *p < 0.05, **p < 0.01, and ****p < 0.0001 indicate significant differences regarding DMSO or Syro, accordingly; ‡‡<p0.01, and ‡‡‡‡p < 0.0001 indicate significant differences between Syro and DMSO.

following experiments.

To evaluate the capacity of Lactrans-1 to transport lactate anions independently of MCTs activity, the MCTs inhibitor Syro was used [26]. Thereby, A549 and HeLa cells were treated with 2.3 and 2.8 μM of Lactrans-1, respectively, and both extra- and intracellular lactate levels were measured in a time-course experiment. As expected, Syro induced intracellular lactate accumulation in both cell lines with a concomitant reduction of extracellular lactate levels compared to DMSO control cells (Fig. 6D). Moreover, Lactrans-1 was able to partially revert the intracellular accumulation of lactate induced by Syro, decreasing these levels especially at 120 and 180 min. Upon Syro, Lactrans-1 was also able to increase extracellular lactate levels surpassing those achieved under control condition with Syro alone (Fig. 6D). When MCTs were not inhibited, intracellular lactate levels of cells treated with Lactrans-1 were maintained low, similar to control cells.

Additional experiments showed that structurally related compounds (Lactrans-4 and −5) but with negligible anionophoric activity in liposome models and minimal cytotoxic potential [25], showed no ability to disturb both extra- and intracellular lactate concentrations compared to DMSO or Syro, supporting the position of both compounds as adequate negative controls (Fig. 7A). In these experiments, Lactrans-1 did not show dose-dependent effect on transporting lactate when cells were treated for 120 min (Fig. 7A); however, it was observed that its potency was quite related to the capacity of these cells to produce lactate.

Lastly, we tested the cytotoxicity of Lactrans-1 in cells where lactate production rate was diminished. For this purpose, both cell lines were starved from glucose 24 h before to replenish them with fresh media containing high (45 mM) or low glucose (1 or 5 mM for A549 and HeLa cells, respectively) in the presence of Lactrans-1 (IC_{75} value). Results showed that after 24 h of treatment cancer cell viability under low glucose conditions was significantly higher than that of cells treated in high glucose medium (Fig. 7B). Quantification of extracellular lactate confirmed that control cells (exposed only to DMSO) cultured in a low glucose medium produced less lactate than cells cultured in high glucose. The less amount of lactate in cells cultured under deprivation conditions correlates with those being less sensitive (recover of cell viability) to this compound (Fig. 7C). Thus, these results suggest that cytotoxicity is increased when a higher lactate concentration is available for facilitated lactate exportation.

3.3. Lactrans-1 deregulates pH homeostasis in cancer cells

Due to the ability of Lactrans-1 to export lactate and other anions such as bicarbonate to a lesser extent [25], a major cellular pH disturbance was expected. Intracellular localization of Lactrans-1 was first evaluated using confocal microscopy. First, a lambda scan analysis showed that the maximum fluorescent emission of this compound was around 520 nm after excitation with a 405 nm laser (data not shown).

Then, by using different organelle trackers, it was possible to determine that Lactrans-1 was highly accumulated in lysosomes of both A549 and HeLa cells after 1 h of treatment (Fig. 8A). This accumulation was observed as soon as 15 min and increased over time (data not

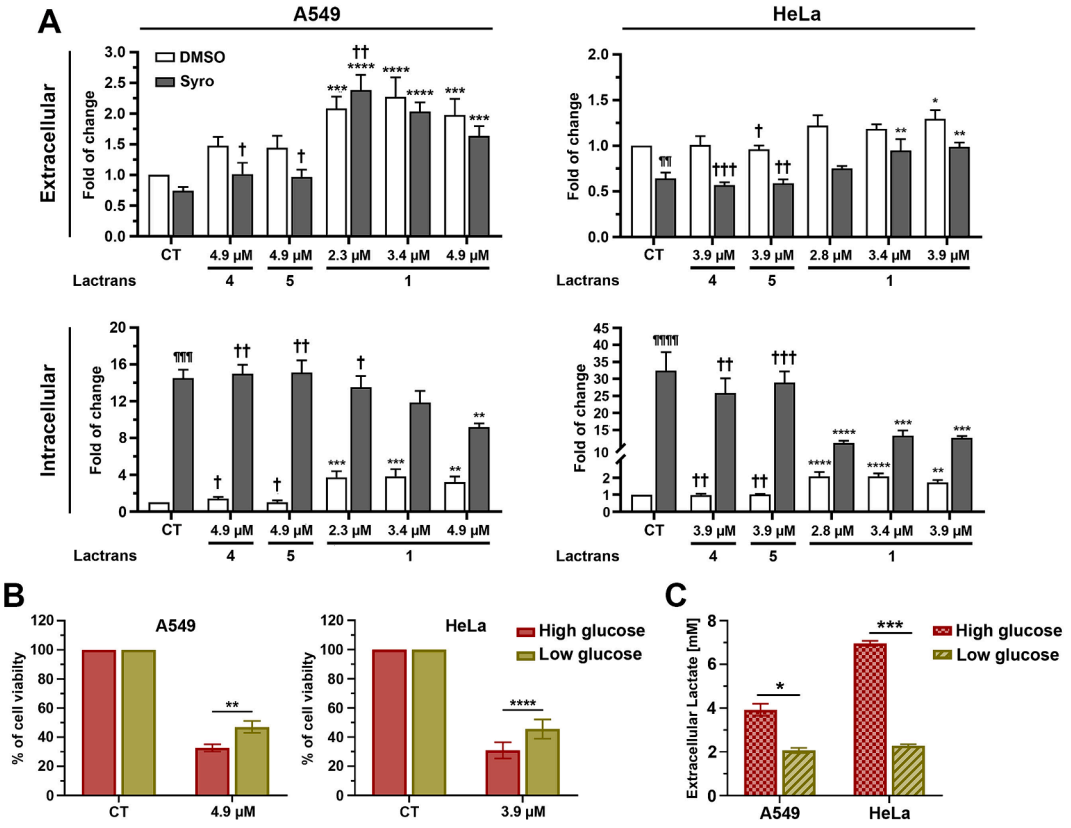

Fig. 7. Lactate determination in A549 and HeLa cells treated with Lactrans-1. **A)** Extra- and intracellular lactate levels were determined in a dose–response experiment treating the cells with different doses of Lactrans-1 for 120 min. A high dose of Lactrans-4 and −5 was also tested. **B)** Cell viability experiments of cells treated with Lactrans-1 under regular and glucose deprivation conditions. Briefly, A549 and HeLa cells were seeded in a low glucose medium (1 mM) and incubated overnight. Next day, they were replenished with fresh media supplemented with high (45 mM) or low glucose (1 mM for A549 and 5 mM for HeLa cells) and after 2 h treated with IC_{75} value of Lactrans-1 for 24 h. The cytotoxic effect of the drug in cells under high and low glucose was compared to their corresponding non-treated cells (CT) considered as 100 % cell viability. **C)** Extracellular lactate quantification of A549 and HeLa control cells only (exposed to DMSO) cultured in regular and glucose deprivation conditions as in B). * $p < 0.05$, ** $p < 0.01$, *** $p < 0.001$ and **** $p < 0.0001$ indicate significant differences regarding DMSO, Syro or control (CT) conditions, accordingly; ¶¶ $p < 0.01$, ¶¶¶ $p < 0.001$, and ¶¶¶¶ $p < 0.0001$ indicate significant differences between Syro and DMSO; † $p < 0.05$, †† $p < 0.01$, and ††† $p < 0.001$ indicate significant differences regarding treatment with 4.9 μM of Lactrans-1 (in the presence of Syro or not).

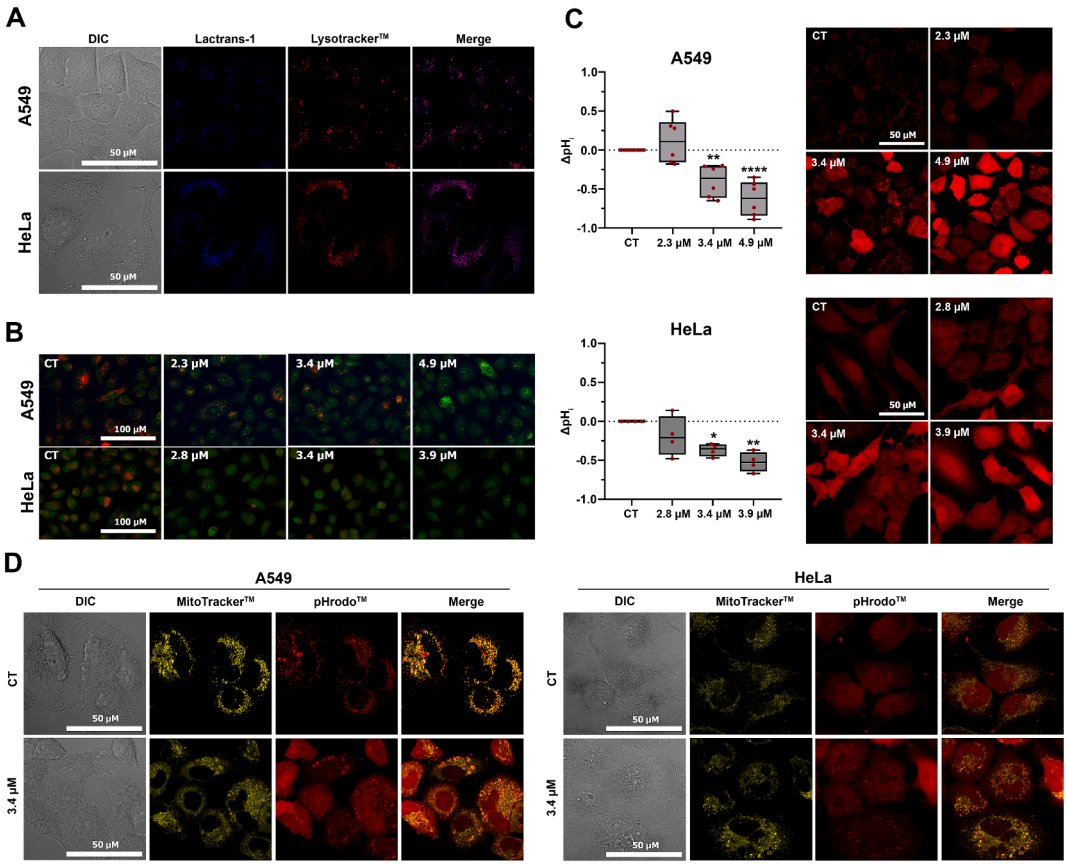

Fig. 8. pH analysis in A549 and HeLa cells treated with Lactrans-1. **A)** Intracellular localization of Lactrans-1 (in blue) in A549 and HeLa cells treated for 1 h with 4.9 and 3.9 µM, respectively. 30 min before image acquisition cells were incubated with LysoTracker™ Red (in red, 50 nM). **B)** Lysosomal pH of A549 and HeLa cells using AO. Cells were treated for 1 h with different doses of Lactrans-1, and then stained with AO (5 µg/mL incubated for 30 min at room temperature). **C)** pH_i of A549 and HeLa cells after 1 h of treatment with different doses of Lactrans-1 and then stained with pHrodo™ Red AM probe. **D)** Mitochondrial acidification analysis in A549 and HeLa cells. Both cell lines were treated with 3.4 µM of Lactrans-1 for 1 h, and then co-incubated with pHrodo™ Red AM probe and MitoTracker™ Deep Red. DIC=differential interference contrast.

shown). Next, the lysosomal pH was evaluated using AO staining and results showed lysosome basification after 1 h of treatment in both cell lines, since the orange fluorescence of the dye almost completely disappeared, especially after high doses (Fig. 8B).

The ability of Lactrans-1 to modify pH_i was also confirmed using the fluorogenic probe pHrodo™ Red AM, which emission intensity increases in acidic milieus. After 1 h of treatment with this compound, a significant drop in pH_i was observed in a dose-dependent manner in both cell lines (Fig. 8C). Confocal microscopy images revealed an increase in the emission of the pHrodo™ probe, not only in the cytosol, but also in unidentified subcellular compartments (Fig. 8C). By using dual staining of pHrodo™ and organelle trackers it was confirmed that in control cells the lysosomes were the main acidic organelles (data not shown), while upon Lactrans-1 treatment, the highest fluorescence intensity co-localized with mitochondrial tracker indicating their acidification (Fig. 8D).

3.4. *Lactrans-1 induces mitochondrial dysfunction and oxidative stress*

Upon Lactrans-1 treatment, different degrees of cytoplasmic vacuolization were observed. While in A549 cells the vacuoles appeared as soon as 1 h of treatment, in HeLa cells these were more evident after 4 h (Fig. 9A, arrows). Hence, by using specific organelle trackers we confirmed that these vacuoles were swelled mitochondria, since the marker was inside or surrounding the vacuoles (Fig. 9B, white arrows). In addition, it was verified that the swelling process was accompanied by a drop in mitochondria membrane potential, as the emission of the CMXRos probe and the shape of mitochondria were lost along time (Fig. 9C).

Mitochondrial dysfunction and pH disturbances have been previously associated with ROS production and activation of oxidative stress-related signaling pathways [21]. Therefore, ROS formation was assessed in cells upon treatment with Lactrans-1 at different times, showing its accumulation and reaching maximum values at 1 h for A549 cells and at 30 min for HeLa cells (Fig. 9D). Interestingly, while in A549 cells ROS levels slightly diminished over time, in Hela cells such levels dropped significantly at 120 min and 240 min. Oxidative stress-related signaling pathways, p38-MAPK and c-Jun N-terminal kinase (JNK/SAPK), were assessed in a longer time-course experiment through western blot. After 1 h of treatment with Lactrans-1, a significant activation of both p38 MAPK and JNK/SAPK pathways was observed (Fig. 9E and F) through the increase in their phosphorylated forms (p-p38 MAPK Thr180/Tyr182 and p-JNK/SAPK Thr183/Tyr185, respectively). Interestingly, the activation of these two pathways was, in general, more prominent in A549 cells than in Hela cells. However, a second greater activation beyond 8 h in both pathways was only observed in HeLa cells.

3.5. *Lactrans-1 displayed synergistic effect with cisplatin in lung cancer cells*

Finally, since combination therapies are a valuable approach frequently used in clinics to increase therapeutic effectiveness and diminish toxicity, we assessed the synergism of Lactrans-1 with the first-line chemotherapeutic agent cisplatin in A549 cells. In these

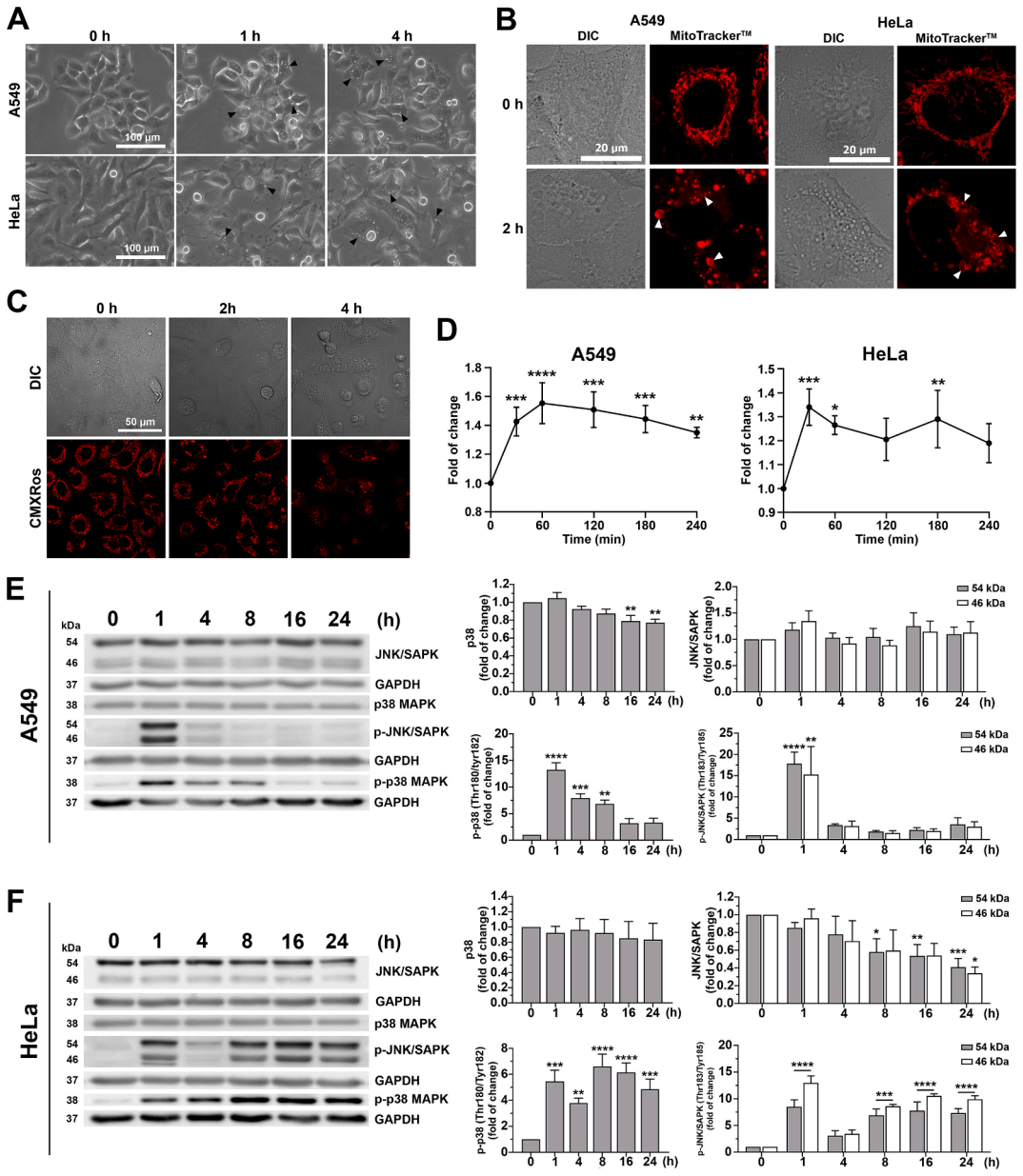

Fig. 9. Cellular stress analysis of A549 and Hela cells treated with Lactrans-1. **A)** Phase contrast images (20X) of cytoplasmic vacuolization in A549 and HeLa cells treated for 0, 1 and 4 h with 4.9 and 3.9 μM of Lactrans-1, respectively. **B)** Mitochondrial swelling in A549 and HeLa cells after 1 h of treatment with 4.9 and 3.9 μM of Lactrans-1, respectively, and then stained with fluorescent marker MitoTracker™ Deep Red (50 nM, 30 min). Images were taken using confocal microscopy. **C)** Mitochondrial membrane potential in A549 cells after 2 and 4 h of treatment with 4.9 μM of Lactrans-1. MitoTracker™ Red CMXRos (5 nM, 15 min) was used to evaluate membrane potential through confocal microscopy. **D)** ROS analysis in A549 and HeLa cells. Cells were treated with 4.9 and 3.9 μM of Lactrans-1, respectively, in a time-course manner up to 240 min. In both experiments, TBHP was used as a positive control. ROS formation was detected by flow cytometry using CellROX® Deep Red Reagent (1 μM, 30 min). **E)** and **F)** Western blot analysis showing protein expression of oxidative stress-related signaling pathways in A549 and HeLa cells, respectively. Cells were treated with Lactrans-1 (4.9 μM for A549 cells and 3.9 μM for HeLa cells) in a time-course manner (up to 24 h). GAPDH expression was used as loading control. The bar graphs represent expression levels (mean ± SEM) of proteins expressed as a fold of change against control (CT). At least three independent experiments were performed. *$p < 0.05$, **$p < 0.01$, ***$p < 0.001$, and ****$p < 0.0001$ indicate significant differences compared to time 0 h.

experiments, cells were treated with different doses of Lactrans-1 (2.3, 3.4 and 4.9 μM) for 4 h and then cisplatin was added (50, 100, 150, 200 and 250 μM) for additional 24 h before cell viability determination through the MTT assay. For all the combinations tested, the CI value was lower than 0.915, indicating that this modality of sequential treatment has a slight to moderate synergistic effect (Fig. 10A and B). Interestingly, the greatest synergistic effect was observed when a low dose of Lactrans-1 (2.3 μM) and cisplatin (100–200 μM) were used (CI≤0.782).

4. Discussion

The implications of lactic acidosis in cancer have been recently rediscovered and their potential to modulate immune response, tumor progression and malignancy has been widely reported [11]. Then, targeting lactate and pH_i homeostasis represent a novel and interesting therapeutic opportunity. In this study, we propose the use of a small-molecule with proven anionophoric activity to effectively disturb lactate permeability across cancer cell membranes and to induce different cell death mechanism through disruption of pH_i homeostasis,

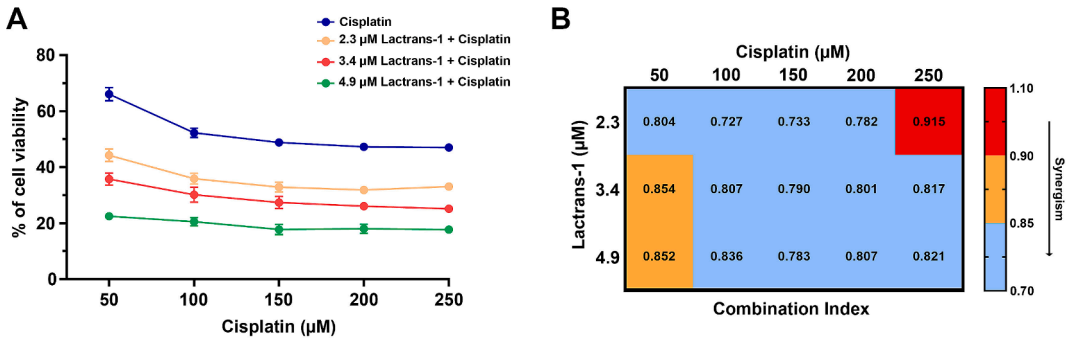

Fig. 10. Analysis of synergism between Lactrans-1 and cisplatin in A549 cells. **A)** Cell viability percentages after 4 h of treatment with Lactrans-1 (2.3, 3.4 and 4.9 μM) and sequential addition of cisplatin. Bars represent mean ± SEM. **B)** Analysis of synergy between Lactrans-1 and cisplatin through determination of CI in the same conditions as in A. Color code: red = additive effect; orange = slight synergic effect; blue = moderate synergic effect.

coupled with the activation of oxidative stress-related signaling pathways.

We were able to demonstrate that Lactrans-1 has shown the ability to effectively reduce cancer cell viability in a wide variety of cell lines including cervix, oral, breast, colon and lung cancer. The toxicity of these newly synthesized click-tambjamine compounds has been related with the transmembrane anion transport capacity that they exhibited in liposomes models [25,27]. These compounds differ from natural tambjamine alkaloids in a 1,2,3-triazole ring that replaces one of the pyrrole groups of the 4-methoxy-2,2′-bipyrrole core [27]. In our case, Lactrans-1 contains an aromatic and an alicyclic fragment linked to the triazole and imine moieties, respectively, which enhanced its anionophoric and cytotoxic activities compared to other derivatives, such as Lactrans-4 and −5, containing different groups [25]. In this manner, Lactrans-1 resulted slightly more potent (displaying lower IC values) than other tambjamine analogues previously reported [21,28].

Our results showed that Lactrans-1 is also able to trigger apoptotic or necrotic cell death depending on the cell line assessed, an effect previously reported with other click-tambjamine analogues [22,29]. A predominant apoptotic cell death evaluated through the activation of the executioner caspase 3 and cleavage of its substrate PARP was observed in HeLa cells after treatment at different time points (beyond 8 h). On the other hand, an early necrotic cell death occurred in A549 cells with a later activation of apoptosis after 24 h of treatment in a different cell subpopulation. Apoptosis is a common cell death mechanism triggered by tambjamine derivatives bearing aromatic enamine substituents [30] or indole-based analogues [21,28].

Lactrans-1 is the first ionophore molecule designed to transport lactate anions with therapeutic applications in the biomedical field. Previously, disruption of lactate shuttling with therapeutic purposes in the context of cancer has been explored by inhibiting either its production or transportation (targeting lactate dehydrogenase −LDH- or MCTs, respectively); however, not all of these approaches have been completely effective, possibly due to the metabolic plasticity of cancer cells [31–33]. The ability of Lactrans-1 to enhance lactate permeability across cellular membranes was studied in two different cancer cell lines because of their distinct glycolytic and lactate production rates. Lactrans-1 was able to partially revert intracellular lactate accumulation, caused by MCTs inhibition using Syro, increasing extracellular lactate concentrations and reducing those inside the cell after few hours of treatment. Moreover, the higher extracellular lactate concentrations after Lactrans-1 treatment compared to DMSO conditions would suggest that this drug is also able to promote indirectly glycolysis. This could be explained by altered steady-state equilibrium of the reaction catalyzed by LDH, favoring lactate formation when the product is removed outside the cell [34,35]. Lactate concentration has been evaluated within this timeframe when cell viability was not significantly affected and the permeability of cell membrane was not compromised, ruling out a toxicity effect in the lactate assessment assays. Moreover, the ability of Lactrans-1 to transport lactate was linked to the cytotoxic effect exhibited in cell viability reversion experiments in which the glycolytic activity of these cells was diminished. Hence, the cytotoxicity elicited by Lactrans-1 was found significantly reduced in both HeLa and A549 cells previously subjected to harmless glucose deprivation conditions in order to lower their lactate production levels. This indicates that the cytotoxic effect of Lactrans-1 could be related to the amount of lactate available to transport, suggesting that highly glycolytic cells might be more affected by this therapeutic strategy.

In cancer cells, the extrusion of protons and other metabolic acidic-end products is essential to avoid chronic intracellular acidification that could impede proper metabolic fluxes necessary for uncontrolled proliferation [36–38]. Minor pH_i changes could affect the activity of multiple proteins and enzymes highly dependent on pH, triggering the collapse of fundamental cellular activities. In the aqueous intracellular milieu, lactic acid is rapidly dissociated into lactate anions and protons ($pK_a \sim 3.9$) reducing pH_i to an acidic steady-state level and representing the main source of challenge for pH_i control [39]. Thus, the rapid production of lactate and protons must be coupled with an efficient symporter system represented mainly by MCTs [16,17]. In our study, the significant drop of pH_i in both cell lines after few hours of treatment could be related to the ability of Lactrans-1 to transport lactate across the plasma membrane uncoupled from protons, facilitating their accumulation inside the cells. Thus, it is feasible to propose that in this scenario, the basal activity of MCTs as lactate and proton-extruders (as well as other related transmembrane proton exporters) in highly glycolytic cancer cells [40] cannot cope with the accumulation of protons derived from the independent lactate exportation caused by Lactrans-1. Our novel approach to disturb lactate permeability uncoupled from proton exportation across cellular membranes, could bypass undesirable effects seen with previous lactate-targeted therapeutic approaches, since pH regulatory mechanisms probably affected by disturbing lactate permeability could trigger a “metabolic catastrophe” hard to reverse [14].

The cytotoxic effect of Lactrans-1 was preceded by a prominent acidification of pH_i that is a key event previously associated with apoptotic cancer cell death [41,42]. Other compounds such as staurosporine [42], camptothecin [43], imidazole [44], somatostatin [45] or ionophores as valinomycin [46] have shown to induce intracellular acidification before activation of executioner caspases [44]. Intracellular acidification has been reported to occur simultaneously to phosphatidylserine externalization during the apoptotic process [47] and is also closely related to mitochondrial dysfunction and stress oxidation [48,49]. This last observation is in accordance with our results showing a concomitant deregulation of organelle pH (such as lysosome and mitochondria) when cells are treated with Lactrans-1. We also reported mitochondrial acidification, which is likely to be related with their functional status indicating membrane potential disruption, increased ROS formation and activation of oxidative stress-related signaling

pathways [50]. We could not elude that Lactrans-1 is able to move other anions like chloride or bicarbonate which are also implicated in the cell homeostasis [25]. This anion movement could be related with the overall pH_i alterations observed here, and could explain the apparent contradictory effect of cytosolic acidification and lysosomal basification under the treatment with Lactrans-1.

Activation of oxidative stress-related signaling pathways is a common effect for several naturally-based and synthetic compounds inducing cancer cell death. The family members of the MAPK pathway, p38-MAPK and JNK/SAPK are especially relevant due to their closely implications with ROS production [51,52]. Depending on the magnitude and duration of stimuli exposure, it has been seen that ROS can induce both adaptive/survival or apoptotic responses [53]. In our study, almost immediately after adding Lactrans-1 there was a significant increase of ROS production in both A549 and HeLa cells, with a simultaneous activation of p38-MAPK and JNK/SAPK signaling pathways. Furthermore, we observed that both cell lines treated with Lactrans-1 showed cytoplasmic vacuolization involving mitochondria; however, in A549 cells their appearance was more acute and prominent than in HeLa cells. Since mitochondria swelling represents a critical damage for the ATP synthesis machinery, this affectation could be related with the differences observed regarding cell death mechanisms, since apoptosis requires energy [54,55]. In addition, the stronger and faster activation of p38-MAPK and JNK/SAPK pathways in cells undergoing necrosis (A549 cells), compared to those cells where apoptosis was first observed (HeLa cells), could indicate how cancer cells respond to the anionophoric effect of Lactrans-1.

Finally, a positive synergistic effect of Lactrans-1 when used in combination with cisplatin was confirmed. The combination of two or more agents to treat cancer may offer the possibility to decrease drug concentrations, reduce undesirable side-effects or even overcome chemoresistance [56]. In our experiments, Lactrans-1 was used as a pretreatment for 4 h before the addition of cisplatin, since major ionic and pH changes were seen early after treatment. In this sequential modality, a moderate synergistic effect was observed after 24 h of treatment. In this manner, our approach consisting in the disruption of lactate homeostasis, targets a different cellular process or signaling pathway, which complements the mechanism of action of cisplatin in proliferative cancer cells, showing the observed synergistic therapeutic effect.

In summary, we have demonstrated that Lactrans-1 facilitates lactate transport in cancer cell membranes and also that the cytotoxicity exhibited correlates well with the amount of lactate transported. Thus, deregulation of lactate permeability, independent of MCTs activity and accompanied by intracellular proton accumulation, resulted in an irreversible disturbance of ionic homeostasis, leading to critical oxidative stress, mitochondrial dysfunction, activation of stress-related signaling pathways and, ultimately, to cancer cell death. Differences observed in the cell death mechanism could rely on intrinsic characteristics of the cell lines used and may be associated to their basal lactate production rates and their ability to cope with osmotic stress. Since the cytotoxicity of our approach showed to be tightly dependent on the available lactate to be transported, we believe that Lactrans-1 could be a promising therapeutic option for highly glycolytic tumors. Furthermore, the synergistic potential displayed in combination with cisplatin makes Lactrans-1 an interesting therapeutic agent to be tested in future *in vivo* studies.

Funding

This work was supported by Consejería de Educación de la Junta de Castilla y León [Project BU067P20] and Ministerio de Ciencia e Innovación [Project PID2020-117610RB-100]. A.A.-B. thanks to PFCHA/Becas Chile (Folio #72200156) for his pre-doctoral scholarship. P.F., D.A.-C. and I.C.-B. thank Consejería de Educación de la Junta de Castilla y León, European Regional Development Fund (ERDF) and European Social Fund (ESF) for their post-doctoral (P.F. and I.C.-B.) and pre-doctoral (D.A.-C.) contracts.

CRediT authorship contribution statement

Alain Arias-Betancur: Writing – original draft, Visualization, Methodology, Investigation, Formal analysis, Data curation. **Pere Fontova:** Writing – review & editing, Visualization, Supervision, Methodology, Investigation, Formal analysis, Data curation. **Daniel Alonso-Carrillo:** Visualization, Methodology, Investigation. **Israel Carreira-Barral:** Writing – review & editing, Visualization, Supervision, Methodology, Investigation. **Janneke Duis:** Visualization, Investigation, Data curation. **María García-Valverde:** Supervision, Resources, Project administration, Funding acquisition. **Vanessa Soto-Cerrato:** Writing – review & editing, Supervision, Resources, Project administration, Funding acquisition. **Roberto Quesada:** Writing – review & editing, Supervision, Resources, Project administration, Funding acquisition, Conceptualization. **Ricardo Pérez-Tomás:** Writing – review & editing, Supervision, Project administration, Funding acquisition, Formal analysis, Conceptualization.

Declaration of competing interest

The authors declare that they have no known competing financial interests or personal relationships that could have appeared to influence the work reported in this paper.

Data availability

The data that support the findings of this study are available from the corresponding author on request.

Acknowledgments

The authors thank the Biology-Bellvitge Unit from Scientific and Technological Centers (CCiTUB), Universitat de Barcelona, and their staff for their support and technical advice.

References

[1] K.G. de la Cruz-López, L.J. Castro-Muñoz, D.O. Reyes-Hernández, A. García-Carrancá, J. Manzo-Merino, Lactate in the regulation of tumor microenvironment and therapeutic approaches, Front. Oncol. 9 (2019) 1143, https://doi.org/10.3389/fonc.2019.01143.

[2] R. Pérez-Tomás, I. Pérez-Guillén, Lactate in the tumor microenvironment: an essential molecule in cancer progression and treatment, Cancers (Basel) 12 (2020) 1–29, https://doi.org/10.3390/cancers12113244.

[3] P. Sonveaux, F. Végran, T. Schroeder, M.C. Wergin, J. Verrax, Z.N. Rabbani, C.J. De Saedeleer, K.M. Kennedy, C. Diepart, B.F. Jordan, M.J. Kelley, B. Gallez, M.L. Wahl, O. Feron, M.W. Dewhirst, Targeting lactate-fueled respiration selectively kills hypoxic tumor cells in mice, J. Clin. Invest. 118 (2008) 3930–3942, https://doi.org/10.1172/JCI36843.

[4] M.G. Vander Heiden, R.J. DeBerardinis, Understanding the intersections between metabolism and cancer biology, Cell. 168 (2017) 657–669, https://doi.org/10.1016/j.cell.2016.12.039.

[5] H. Wu, Z. Ding, D. Hu, F. Sun, C. Dai, J. Xie, X. Hu, Central role of lactic acidosis in cancer cell resistance to glucose deprivation-induced cell death, J. Pathol. 227 (2012) 189–199, https://doi.org/10.1002/path.3978.

[6] H. Wu, M. Ying, X. Hu, Lactic acidosis switches cancer cells from aerobic glycolysis back to dominant oxidative phosphorylation, Oncotarget 7 (2016) 40621–40629, https://doi.org/10.18632/oncotarget.9746.

[7] J. Xie, H. Wu, C. Dai, Q. Pan, Z. Ding, D. Hu, B. Ji, Y. Luo, X. Hu, Beyond Warburg effect - Dual metabolic nature of cancer cells, Sci. Rep. 4 (2014) 4927, https://doi.org/10.1038/srep04927.

[8] L.K. Boroughs, R.J. Deberardinis, Metabolic pathways promoting cancer cell survival and growth, Nat. Cell Biol. 17 (2015) 351–359, https://doi.org/10.1038/ncb3124.

[9] C.A. Lyssiotis, A.C. Kimmelman, Metabolic interactions in the tumor microenvironment, Trends Cell Biol. 27 (2017) 863–875, https://doi.org/10.1016/j.tcb.2017.06.003.

[10] I. Dagogo-Jack, A.T. Shaw, Tumour heterogeneity and resistance to cancer therapies, Nat. Rev. Clin. Oncol. 15 (2018) 81–94, https://doi.org/10.1038/nrclinonc.2017.166.

[11] L. Ippolito, A. Morandi, E. Giannoni, P. Chiarugi, Lactate: a metabolic driver in the tumour landscape, Trends Biochem. Sci. 44 (2019) 153–166, https://doi.org/10.1016/j.tibs.2018.10.011.
[12] R. Boidot, F. Vegran, A. Meulle, A. Le Breton, C. Dessy, P. Sonveaux, S. Lizard-Nacol, O. Feron, Regulation of monocarboxylate transporter MCT1 expression by p53 mediates inward and outward lactate fluxes in tumors, Cancer Res. 72 (2012) 939–948, https://doi.org/10.1158/0008-5472.CAN-11-2474.
[13] J.R. Casey, S. Grinstein, J. Orlowski, Sensors and regulators of intracellular pH, Nat. Rev. Mol. Cell Biol. 11 (2010) 50–61, https://doi.org/10.1038/nrm2820.
[14] S.K. Parks, J. Chiche, J. Pouysségur, Disrupting proton dynamics and energy metabolism for cancer therapy, Nat. Rev. Cancer. 13 (2013) 611–623, https://doi.org/10.1038/nrc3579.
[15] P. Swietach, What is pH regulation, and why do cancer cells need it? Cancer Metastasis Rev. 38 (2019) 5–15, https://doi.org/10.1007/s10555-018-09778-x.
[16] B.J. Czowski, R. Romero-Moreno, K.J. Trull, K.A. White, Cancer and pH dynamics: transcriptional regulation, proteostasis, and the need for new molecular tools, Cancers (Basel) 12 (2020) 1–19, https://doi.org/10.3390/cancers12102760.
[17] B.A. Webb, M. Chimenti, M.P. Jacobson, D.L. Barber, Dysregulated pH: a perfect storm for cancer progression, Nat. Rev. Cancer 11 (2011) 671–677, https://doi.org/10.1038/nrc3110.
[18] R. Polanski, C.L. Hodgkinson, A. Fusi, D. Nonaka, L. Priest, P. Kelly, F. Trapani, P. W. Bishop, A. White, S.E. Critchlow, P.D. Smith, F. Blackhall, C. Dive, C.J. Morrow, Activity of the monocarboxylate transporter 1 inhibitor azd3965 in small cell lung cancer, Clin. Cancer Res. 20 (2014) 926–937, https://doi.org/10.1158/1078-0432.CCR-13-2270.
[19] R.A. Noble, N. Bell, H. Blair, A. Sikka, H. Thomas, N. Phillips, S. Nakjang, S. Miwa, R. Crossland, V. Rand, D. Televantou, A. Long, H.C. Keun, C.M. Bacon, S. Bomken, S.E. Critchlow, S.R. Wedge, Inhibition of monocarboxyate transporter 1 by AZD3965 as a novel therapeutic approach for diffuse large B-cell lymphoma and burkitt lymphoma, Haematologica 102 (2017) 1247–1257, https://doi.org/10.3324/haematol.2016.163030.
[20] D.Y. Lee, J.H. Ha, M. Kang, Z. Yang, W. Jiang, B.Y.S. Kim, Strategies of perturbing ion homeostasis for cancer therapy, Adv. Ther. (Weinh) 5 (2022) 2100189, https://doi.org/10.1002/adtp.202100189.
[21] P. Manuel-Manresa, L. Korrodi-Gregório, E. Hernando, A. Villanueva, D. Martínez-García, A.M. Rodilla, R. Ramos, M. Fardilha, J. Moya, R. Quesada, V. Soto-Cerrato, R. Pérez-Tomás, Novel indole-based tambjamine-analogues induce apoptotic lung cancer cell death through p38 mitogen-activated protein kinase activation, Mol. Cancer Ther. 16 (2017) 1224–1235, https://doi.org/10.1158/1535-7163.MCT-16-0752.
[22] A.M. Rodilla, L. Korrodi-Gregório, E. Hernando, P. Manuel-Manresa, R. Quesada, R. Pérez-Tomás, V. Soto-Cerrato, Synthetic tambjamine analogues induce mitochondrial swelling and lysosomal dysfunction leading to autophagy blockade and necrotic cell death in lung cancer, Biochem. Pharmacol. 126 (2017) 23–33, https://doi.org/10.1016/j.bcp.2016.11.022.
[23] T. Yan, X. Zheng, S. Liu, Y. Zou, J. Liu, Ion transporters: emerging agents for anticancer therapy, Sci. China Chem. 65 (2022) 1265–1278, https://doi.org/10.1007/s11426-022-1258-4.
[24] S.K. Ko, S.K. Kim, A. Share, V.M. Lynch, J. Park, W. Namkung, W. Van Rossom, N. Busschaert, P.A. Gale, J.L. Sessler, I. Shin, Synthetic ion transporters can induce apoptosis by facilitating chloride anion transport into cells, Nat. Chem. 6 (2014) 885–892, https://doi.org/10.1038/nchem.2021.
[25] D. Alonso-Carrillo, A. Arias-Betancur, I. Carreira-Barral, P. Fontova, V. Soto-Cerrato, M. García-Valverde, R. Pérez-Tomás, R. Quesada, Small molecule anion carriers facilitate lactate transport in model liposomes and cells, IScience 26 (2023) 107898, https://doi.org/10.1016/j.isci.2023.107898.
[26] D. Benjamin, D. Robay, S.K. Hindupur, J. Pohlmann, M. Colombi, M.Y. El-Shemerly, S.M. Maira, C. Moroni, H.A. Lane, M.N. Hall, Dual inhibition of the lactate transporters MCT1 and MCT4 is synthetic lethal with metformin due to NAD+ depletion in cancer cells, Cell Rep. 25 (2018) 3047–3058.e4, https://doi.org/10.1016/j.celrep.2018.11.043.
[27] I. Carreira-Barral, M. Mielczarek, D. Alonso-Carrillo, V. Capurro, V. Soto-Cerrato, R. Pérez Tomás, E. Caci, M. García-Valverde, R. Quesada, Click-tambjamines as efficient and tunable bioactive anion transporters, ChemComm. 56 (2020) 3218–3221, https://doi.org/10.1039/d0cc00643b.
[28] D. Martínez-García, M. Pérez-Hernández, L. Korrodi-Gregório, R. Quesada, R. Ramos, N. Baixeras, R. Pérez-Tomás, V. Soto-Cerrato, The natural-based antitumor compound T21 decreases survivin levels through potent stat3 inhibition in lung cancer models, Biomolecules 9 (2019) 361, https://doi.org/10.3390/biom9080361.
[29] A. Molero-Valenzuela, P. Fontova, D. Alonso-Carrillo, I. Carreira-Barral, A. A. Torres, M. García-Valverde, C. Benítez-García, R. Pérez-Tomás, R. Quesada, V. Soto-Cerrato, A novel late-stage autophagy inhibitor that efficiently targets lysosomes inducing potent cytotoxic and sensitizing effects in lung cancer, Cancers (Basel) 14 (2022) 3387, https://doi.org/10.3390/cancers14143387.
[30] E. Hernando, V. Soto-Cerrato, S. Cortés-Arroyo, R. Pérez-Tomás, R. Quesada, Transmembrane anion transport and cytotoxicity of synthetic tambjamine analogs, Org. Biomol. Chem. 12 (2014) 1771–1778, https://doi.org/10.1039/c3ob42341g.
[31] D. Benjamin, M. Colombi, S.K. Hindupur, C. Betz, H.A. Lane, M.Y.M. El-Shemerly, M. Lu, L. Quagliata, L. Terracciano, S. Moes, T. Sharpe, A. Wodnar-Filipowicz, C. Moroni, M.N. Hall, Syrosingopine sensitizes cancer cells to killing by metformin, Sci. Adv. 2 (2016) e1601756, https://doi.org/10.1126/sciadv.1601756.
[32] M. Maeda, M. Ko, M.M. Mane, I.J. Cohen, M. Shindo, K. Vemuri, I. Serganova, R. Blasberg, Genetic and Drug inhibition of LDH-A: effects on murine gliomas, Cancers (Basel) 14 (2022) 2306, https://doi.org/10.3390/cancers14092306.
[33] N. Oshima, R. Ishida, S. Kishimoto, K. Beebe, J.R. Brender, K. Yamamoto, D. Urban, G. Rai, M.S. Johnson, G. Benavides, G.L. Squadrito, D. Crooks, J. Jackson, A. Joshi, B.T. Mott, J.H. Shrimp, M.A. Moses, M.J. Lee, A. Yuno, T.D. Lee, X. Hu, T. Anderson, D. Kusewitt, H.H. Hathaway, A. Jadhav, D. Picard, J.B. Trepel, J. B. Mitchell, G.M. Stott, W. Moore, A. Simeonov, L.A. Sklar, J.P. Norenberg, W. M. Linehan, D.J. Maloney, C.V. Dang, A.G. Waterson, M. Hall, V.M. Darley-Usmar, M.C. Krishna, L.M. Neckers, Dynamic imaging of LDH inhibition in tumors reveals rapid in vivo metabolic rewiring and vulnerability to combination therapy, Cell Rep. 30 (2020) 1798–1810.e4, https://doi.org/10.1016/j.celrep.2020.01.039.
[34] M.J. Rogatzki, B.S. Ferguson, M.L. Goodwin, L.B. Gladden, Lactate is always the end product of glycolysis, Front. Neurosci. 9 (2015), https://doi.org/10.3389/fnins.2015.00022.
[35] M.J. Lambeth, M.J. Kushmerick, A computational model for glycogenolysis in skeletal muscle, Ann. Biomed. Eng. 30 (2002) 808–827, https://doi.org/10.1114/1.1492813.
[36] A.P. Andersen, J.M.A. Moreira, S.F. Pedersen, Interactions of ion transporters and channels with cancer cell metabolism and the tumour microenvironment, Philos. Trans. R. Soc. Lond. B. Biol. Sci. 369 (2014), https://doi.org/10.1098/rstb.2013.0098.
[37] R.A. Gatenby, R.J. Gillies, Why do cancers have high aerobic glycolysis? Nat. Rev. Cancer. 4 (2004) 891–899, https://doi.org/10.1038/nrc1478.
[38] M.V. Liberti, J.W. Locasale, The Warburg effect: how does it benefit cancer cells? Trends Biochem. Sci. 41 (2016) 211–218, https://doi.org/10.1016/j.tibs.2015.12.001.
[39] P. Swietach, E. Boedtkjer, S.F. Pedersen, How protons pave the way to aggressive cancers, Nat. Rev. Cancer. 23 (2023) 825–841, https://doi.org/10.1038/s41568-023-00628-9.
[40] N. Draoui, O. Feron, Lactate shuttles at a glance: from physiological paradigms to anti-cancer treatments, Dis. Model. Mech. 4 (2011) 727–732, https://doi.org/10.1242/dmm.007724.
[41] D. Lagadic-Gossmann, L. Huc, V. Lecureur, Alterations of intracellular pH homeostasis in apoptosis: origins and roles, Cell Death Differ. 11 (2004) 953–961, https://doi.org/10.1038/sj.cdd.4401466.
[42] T.F. Sergeeva, M.V. Shirmanova, O.A. Zlobovskaya, A.I. Gavrina, V.V. Dudenkova, M.M. Lukina, K.A. Lukyanov, E.V. Zagaynova, Relationship between intracellular pH, metabolic co-factors and caspase-3 activation in cancer cells during apoptosis, Biochim. Biophys. Acta Mol. Cell Res. 2017 (1864) 604–611, https://doi.org/10.1016/j.bbamcr.2016.12.022.
[43] V. Goossens, J. Grooten, K. De Vos, W. Fiers, Direct evidence for tumor necrosis factor-induced mitochondrial reactive oxygen intermediates and their involvement in cytotoxicity, Proc. Natl. Acad. Sci. 92 (1995) 8115–8119, https://doi.org/10.1073/pnas.92.18.8115.
[44] K. Iguchi, S. Usui, R. Ishida, K. Hirano, Imidazole-induced cell death, associated with intracellular acidification, caspase-3 activation, DFF-45 cleavage, but not oligonucleosomal DNA fragmentation, Apoptosis 7 (2002) 519–525, https://doi.org/10.1023/A:1020691026578.
[45] D. Liu, G. Martino, M. Thangaraju, M. Sharma, F. Halwani, S.-H. Shen, Y.C. Patel, C.B. Srikant, Caspase-8-mediated intracellular acidification precedes mitochondrial dysfunction in somatostatin-induced apoptosis, J. Biol. Chem. 275 (2000) 9244–9250, https://doi.org/10.1074/jbc.275.13.9244.
[46] I.J. Furlong, C. Lopez Mediavilla, R. Ascaso, A.L. Rivas, M.K.L. Collins, Induction of apoptosis by valinomycin: mitochondrial permeability transition causes intracellular acidification, Cell Death Differ. 5 (1998) 214–221, https://doi.org/10.1038/sj.cdd.4400335.
[47] G.W. Meisenholder, S.J. Martin, D.R. Green, J. Nordberg, B.M. Babior, R. A. Gottlieb, Events in apoptosis: acidification is downstream of protease activation and BCL-2 protection, J. Biol. Chem. 271 (1996) 16260–16262, https://doi.org/10.1074/jbc.271.27.16260.
[48] S. Matsuyama, J. Llopis, Q.L. Deveraux, R.Y. Tsien, J.C. Reed, Changes in intramitochondrial and cytosolic pH: early events that modulate caspase activation during apoptosis, Nat. Cell Biol. 2 (2000) 318–325, https://doi.org/10.1038/35014006.
[49] M.-C. Gendron, N. Schrantz, D. Métivier, G. Kroemer, Z. Maciorowskar, F. Sureau, S. Koester, P.X. Petit, Oxidation of pyridine nucleotides during Fas-and ceramide-induced apoptosis in Jurkat cells: correlation with changes in mitochondria, glutathione depletion, intracellular acidification and caspase 3 activation, Biochem. J. 353 (2001) 357–367, https://doi.org/10.1042/bj3530357.
[50] J. Santo-Domingo, N. Demaurex, The renaissance of mitochondrial pH, J. Gen. Physiol. 139 (2012) 415–423, https://doi.org/10.1085/jgp.201110767.
[51] B. Canovas, A.R. Nebreda, Diversity and versatility of p38 kinase signalling in health and disease, Nat. Rev. Mol. Cell Biol. 22 (2021) 346–366, https://doi.org/10.1038/s41580-020-00322-w.
[52] H.M. Shen, Z.G. Liu, JNK signaling pathway is a key modulator in cell death mediated by reactive oxygen and nitrogen species, Free Radic. Biol. Med. 40 (2006) 928–939, https://doi.org/10.1016/j.freeradbiomed.2005.10.056.

[53] J. McCubrey, M. LaHair, R. Franklin, Reactive Oxygen species-induced activation of the MAP kinase signaling pathways, Antioxid. Redox Signal. 8 (2006) 1775–1789, https://doi.org/10.1089/ars.2006.8.1775.
[54] A.L. Edinger, C.B. Thompson, Death by design: apoptosis, necrosis and autophagy, Curr. Opin. Cell Biol. 16 (2004) 663–669, https://doi.org/10.1016/j.ceb.2004.09.011.
[55] A.V. Shubin, I.V. Demidyuk, A.A. Komissarov, L.M. Rafieva, S.V. Kostrov, Cytoplasmic vacuolization in cell death and survival, Oncotarget 7 (2016) 55863–55889, https://doi.org/10.18632/oncotarget.10150.
[56] P. Jaaks, E.A. Coker, D.J. Vis, O. Edwards, E.F. Carpenter, S.M. Leto, L. Dwane, F. Sassi, H. Lightfoot, S. Barthorpe, D. van der Meer, W. Yang, A. Beck, T. Mironenko, C. Hall, J. Hall, I. Mali, L. Richardson, C. Tolley, J. Morris, F. Thomas, E. Lleshi, N. Aben, C.H. Benes, A. Bertotti, L. Trusolino, L. Wessels, M. J. Garnett, Effective drug combinations in breast, colon and pancreatic cancer cells, Nature 603 (2022) 166–173, https://doi.org/10.1038/s41586-022-04437-2.